

# Selectivity and Anti-Parkinson's Potential of Thiadiazolidinone RGS4 Inhibitors

Levi L. Blazer,<sup>\*,†</sup> Andrew J. Storaska,<sup>†,‡</sup> Emily M. Jutkiewicz,<sup>†</sup> Emma M. Turner,<sup>§</sup> Mariangela Calcagno,<sup>||</sup> Susan M. Wade,<sup>†</sup> Qin Wang,<sup>†</sup> Xi-Ping Huang,<sup>⊥</sup> John R. Traynor,<sup>†</sup> Stephen M. Husbands,<sup>§</sup> Michele Morari,<sup>||</sup> and Richard R. Neubig<sup>‡</sup>

<sup>†</sup>Department of Pharmacology, University of Michigan Medical School, Ann Arbor, Michigan 48109, United States,

<sup>‡</sup>Department of Pharmacology and Toxicology, Michigan State University, East Lansing, Michigan 48824, United States

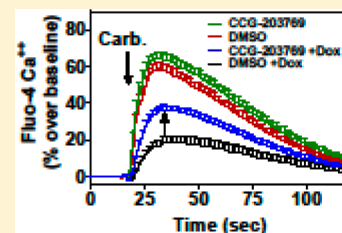
<sup>§</sup>Department of Pharmacy and Pharmacology, University of Bath, Bath, U.K.

<sup>||</sup>Section of Pharmacology, Department of Medical Science, University of Ferrara, Ferrara, Italy 44121

<sup>⊥</sup>National Institute of Mental Health Psychoactive Drug Screening Program (NIMH PDSP), Department of Pharmacology, University of North Carolina, Chapel Hill, North Carolina 27599, United States

## Supporting Information

**ABSTRACT:** Many current therapies target G protein coupled receptors (GPCR), transporters, or ion channels. In addition to directly targeting these proteins, disrupting the protein–protein interactions that localize or regulate their function could enhance selectivity and provide unique pharmacologic actions. Regulators of G protein signaling (RGS) proteins, especially RGS4, play significant roles in epilepsy and Parkinson's disease. Thiadiazolidinone (TDZD) inhibitors of RGS4 are nanomolar potency blockers of the biochemical actions of RGS4 *in vitro*. Here, we demonstrate the substantial selectivity (8- to >5000-fold) of CCG-203769 for RGS4 over other RGS proteins. It is also 300-fold selective for RGS4 over GSK-3 $\beta$ , another target of this class of chemical scaffolds. It does not inhibit the cysteine protease papain at 100  $\mu$ M. CCG-203769 enhances G $\alpha_q$ -dependent cellular Ca<sup>2+</sup> signaling in an RGS4-dependent manner. TDZD inhibitors also enhance G $\alpha_i$ -dependent  $\delta$ -OR inhibition of cAMP production in SH-SY-5Y cells, which express endogenous receptors and RGS4. Importantly, CCG-203769 potentiates the known RGS4 mechanism of G $\alpha_i$ -dependent muscarinic bradycardia *in vivo*. Furthermore, it reverses raclopride-induced akinesia and bradykinesia in mice, a model of some aspects of the movement disorder in Parkinson's disease. A broad assessment of compound effects revealed minimal off-target effects at concentrations necessary for cellular RGS4 inhibition. These results expand our understanding of the mechanism and specificity of TDZD RGS inhibitors and support the potential for therapeutic targeting of RGS proteins in Parkinson's disease and other neural disorders.



**KEYWORDS:** Regulator of G-protein signaling, Parkinson's disease, PPI, RGS, protein–protein interaction, thiadiazolidinone

The G protein-coupled receptors (GPCRs) remain key drug targets for therapeutic use.<sup>1–3</sup> The recent crystal structures of numerous GPCRs have improved the ability to develop subtype-selective ligands.<sup>4,5</sup> Also, allosteric modulators of GPCRs have provided new degrees of control of signaling with the potential for more refined therapeutic agents.<sup>2,6</sup> In some cases, however, a single GPCR may mediate both desired and unwanted actions. This is especially true for agonists (e.g., clonidine and adenosine) active in the central nervous system (CNS) where side effects are major limitations to use. It would be highly advantageous to have a mechanism to improve the selectivity of existing GPCR ligands. The downstream actions of GPCRs are modulated by the family of regulator of G protein signaling proteins (RGS proteins). Many of the 20 members of this family are abundantly expressed in the brain.<sup>7–13</sup> Consequently, they have been proposed as intriguing CNS drug targets.<sup>7–13</sup> RGS proteins act intracellularly by speeding the deactivation of G $\alpha_i$  and G $\alpha_q$  family G proteins. Inhibition of RGS proteins would thus be expected to

potentiate the actions of GPCR agonists. Furthermore, the differential tissue distribution of RGS proteins could provide a novel way to selectively enhance GPCR agonist action in a tissue-specific or neuron-subtype-specific manner.

RGS4, in particular, assembles in a complex with A1 adenosine receptors and has been proposed to suppress the anticonvulsant action of adenosine.<sup>14</sup> Suppression of RGS4 also mediates long-term depression by dopamine through D2 receptors in medium spiny neurons,<sup>15</sup> and RGS4 knockout mice have reduced impairment in 6-OHDA mouse models.<sup>15</sup> Furthermore, loss of RGS4 appears to suppress abnormal involuntary movements in mice which represents a model for DOPA-induced dyskinesias.<sup>16</sup> According to the recent model,<sup>15</sup> a key action of dopamine is to suppress RGS4 function. Thus,

Received: February 13, 2015

Revised: April 4, 2015

Published: April 6, 2015

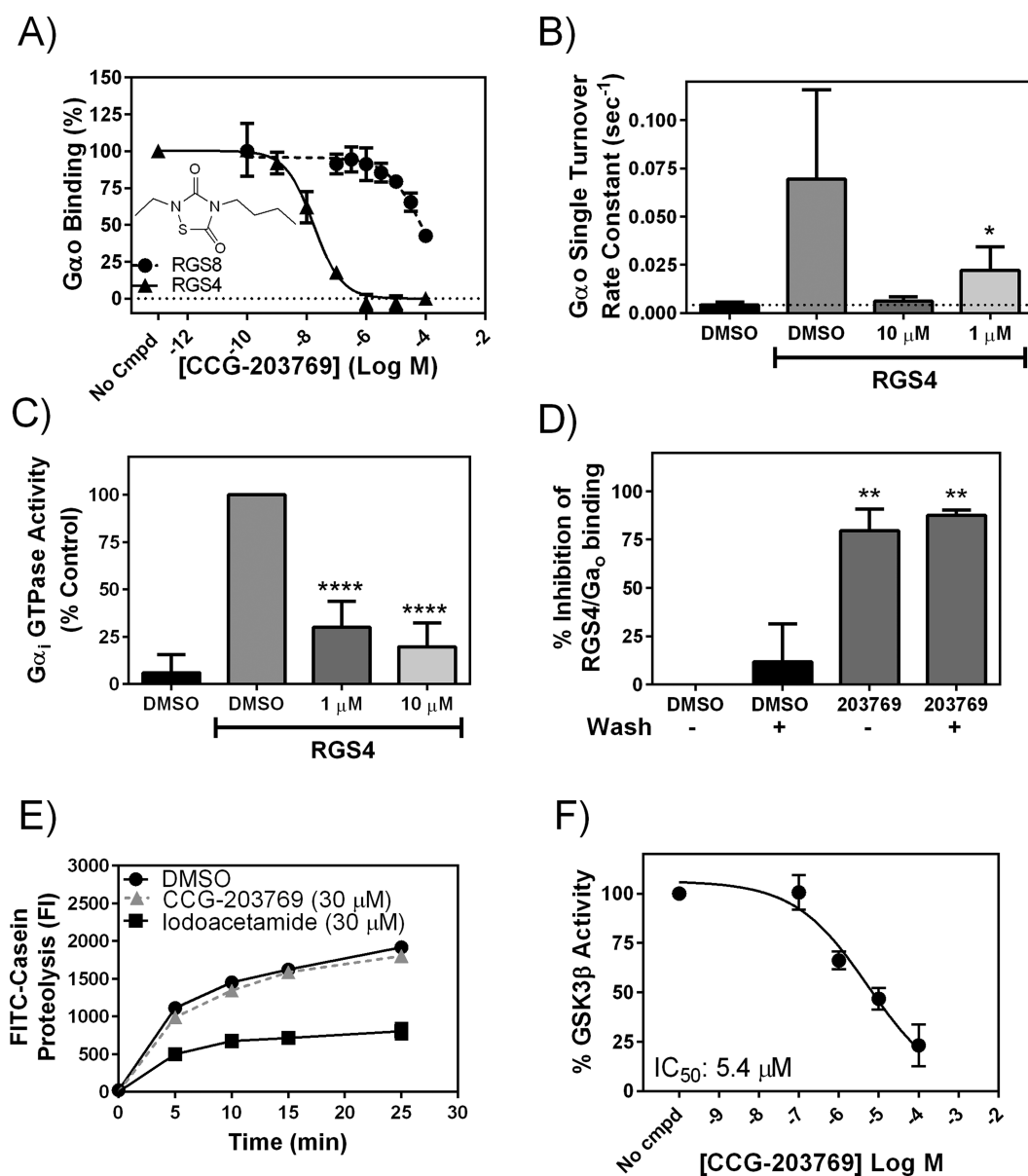


**Figure 1.** Biochemical characterization of RGS inhibitors. (A) CCG-203769 inhibits RGS4 and RGS8 binding to  $G\alpha_o$  in FCPIA in a concentration-dependent manner. Inset: chemical structure of CCG-203769. See Table 1 for IC<sub>50</sub> values. CCG-203769 inhibits the RGS-mediated acceleration of GTPase activity by both (B)  $G\alpha_o$  in single-turnover and (C)  $G\alpha_{i1}$  in steady-state GTPase assays. (D) CCG-203769 irreversibly inhibits RGS4 binding to  $G\alpha_o$  in nonreducing buffers. RGS4-coated beads were treated with 0.5  $\mu$ M CCG-203769, extensively washed, and then probed for  $G\alpha_o$  binding. (E) CCG-203769 (30  $\mu$ M) does not inhibit the cysteine protease papain. The positive control compound, iodoacetamide (30  $\mu$ M) did effectively inhibit papain activity (see Methods for details). (F) CCG-203769 inhibits GSK-3 $\beta$  with an IC<sub>50</sub> value of 5  $\mu$ M. Data are presented as the mean  $\pm$  SEM from at least three independent experiments. \*  $p < 0.05$ , \*\*\*\* $p < 0.0001$ .

direct, chemical inhibition of the hyperactive RGS4 would eliminate the need for dopamine and could provide a novel dopamine-independent approach to Parkinson's disease. Consequently, therapeutic targeting of RGS4 could be of great interest.

It has been challenging to effectively disrupt RGS4/ $G\alpha$  and other protein–protein interactions, especially in the CNS, but progress is being made.<sup>17–19</sup> Indeed, the emerging consensus in the field is that effective inhibitors of protein–protein interactions (iPPIs) may not meet the “standard” pharmaceutical criteria for drug-like molecules.<sup>20,21</sup> In spite of this, numerous compounds with MW > 500<sup>20–22</sup> and several covalent protein modifiers<sup>23,24</sup> are now in clinical trials. We recently described a series of nanomolar-potency TDZD

inhibitors of RGS proteins<sup>25,26</sup> that can disrupt RGS4 binding to  $G\alpha$  subunits in HEK-293 cells. As is seen for some other potent iPPIs, they covalently modify cysteine residues in RGS proteins,<sup>25</sup> but, surprisingly, they have high specificity for RGS4 vs other cysteine-dependent proteins such as some kinases and cysteine proteases.

In this study, we assess the specificity of TDZD RGS4 inhibitors and demonstrate cellular activity on RGS4 actions on  $G\alpha_q$ -mediated cellular Ca<sup>2+</sup> signaling and delta-opioid regulation of adenylyl cyclase. Furthermore, CCG-203769 shows *in vivo* activity on muscarinic control of heart rate as well as in reversing raclopride-induced Parkinson's-like effects. These results represent the first demonstration of *in vivo* effects of

TDZD RGS4 inhibitors and implicate a potential role in Parkinson's disease and other neuropsychiatric disorders.

## RESULTS AND DISCUSSION

Identifying selective small molecule inhibitors of protein–protein interactions with activity in the central nervous system remains a key challenge to the expansion of the current therapeutic repertoire beyond receptors, transporters, and kinases. Our previously described RGS4 inhibitor CCG-203769 blocks the RGS4- $G\alpha_o$  protein–protein interaction *in vitro* with an  $IC_{50}$  value of 17 nM in the flow cytometry protein interaction assay (FCPIA, Figure 1A). More importantly, it also displays dramatic selectivity for RGS4 over other RGS proteins (Table 1). The closely related RGS8 is very weakly inhibited

**Table 1. Selectivity of CCG-203769<sup>a</sup>**

RGS protein	$IC_{50}$ ( $\mu$ M)	fold selectivity (RGS4)
RGS4	0.017	1
RGS19	0.14	8.2
RGS16	6	350
RGS8	79	4650
RGS7	>100	>6000
GSK3 $\beta$	5.4	320
papain	>100	>6000

<sup>a</sup>The binding of RGS proteins to  $G\alpha_o$  was measured using FCPIA. CCG-203769 inhibited RGS/ $G\alpha_o$  binding in an RGS-selective manner. Functional data for non-RGS activities are described in the text. Data are presented as the mean from three independent experiments performed in duplicate. Fold-selectivity is presented as the ratio of the  $IC_{50}$  of CCG-203769 toward a given target versus its  $IC_{50}$  against RGS4.

( $IC_{50}$  >60  $\mu$ M) providing >4500-fold selectivity for RGS4 (Figure 1A and Table 1). This difference is greater than that seen for our earlier TDZD inhibitor, CCG-50014, which was only ~350-fold selective for RGS4 over RGS8.<sup>25,26</sup> CCG-203769 inhibits RGS19 with an  $IC_{50}$  of 140 nM (8-fold selective for RGS4) and 6  $\mu$ M for RGS16 (350-fold). As with previously reported RGS4 inhibitors, CCG-203769 does not inhibit RGS7, which lacks cysteines in the RGS domain (Table 1).

In addition to inhibiting RGS4/ $G\alpha$  binding, CCG-203769 also blocks the GTPase accelerating protein (GAP) activity of RGS4. In single-turnover and steady-state GTPase experiments with  $G\alpha_o$  and  $G\alpha_{i1}$ , the rate of GTP hydrolysis is strongly stimulated by RGS4, and this effect is inhibited by CCG-203769 with an  $IC_{50}$  < 1  $\mu$ M (Figure. 1B,C). As previously shown for the related TDZD compound CCG-50014,<sup>25</sup> our new compound is irreversible in nonreducing buffers (Figure 1D). This, as well as the complete lack of effect on RGS7, is consistent with CCG-203769 having the same thiol-modification mechanism as CCG-50014.<sup>25</sup>

Beyond RGS protein specificity, CCG-203769 is highly selective for RGS4 vs other thiol-dependent proteins. To assess effects on a protein with a catalytic cysteine residue, we tested CCG-203769 for inhibition of the cysteine protease papain. The general thiol-reactive reagent iodoacetamide strongly inhibited papain-mediated hydrolysis of the fluorescent casein substrate at 30  $\mu$ M. CCG-203769 at the same concentration had no effect on the protease activity of papain (Figure 1E).

Related TDZD compounds are inhibitors of glycogen synthase kinase 3 $\beta$ .<sup>27–29</sup> Indeed, they are currently being evaluated in clinical trials for depression and Alzheimer's disease based on this proposed mechanism. Using a radiometric assay, we show that CCG-203769 inhibits GSK-3 $\beta$  with an  $IC_{50}$  value of 5  $\mu$ M (Figure 1F). This represents 300-fold selectivity of our compound for RGS4 vs GSK-3 $\beta$ .

The nanomolar potency on RGS4 *in vitro* translates to respectable cellular activity. We first examined the RGS4/ $G\alpha_o$  interaction in HEK293 cells. RGS4 is typically present in the cytoplasm but translocates to the membrane when coexpressed with a  $G\alpha$  subunit as demonstrated previously.<sup>25</sup> Similar to prior results with CCG-50014,<sup>25</sup> CCG-203769 also reverses the  $G\alpha_o$ -induced membrane translocation of GFP-tagged RGS4 (Figure 2). This demonstrates inhibition of the RGS4- $G\alpha_o$  interaction in cells. The functional consequences of CCG-203769 were further investigated using a controlled system where induced expression of RGS4 suppresses  $G\alpha_q$ -mediated  $Ca^{2+}$  signaling activated by the M3 muscarinic receptor. Doxycycline treatment induces RGS4 expression (Figure S1A, Supporting Information) reducing the  $Ca^{2+}$  transient induced by 1 nM carbachol by 63% (Figures S1B and C and 3A, Supporting Information). At concentrations of 1 and 3  $\mu$ M, CCG-203769 has no effect on intracellular  $Ca^{2+}$  responses to carbachol stimulation of the M3 muscarinic receptor in the absence of RGS4. However, at the same concentrations, it partially reverses the RGS4-mediated muscarinic suppression. At higher concentrations, there may be an off-target effect as the compound appears to inhibit the  $Ca^{2+}$  transient induced by carbachol. This is similar to previously observed, though more dramatic, effects of CCG-50014 to disrupt  $Ca^{2+}$  handling in HEK cells.<sup>26</sup>

We used SH-SY-5Y neuroblastoma cells to study endogenously expressed RGS and opioid receptors. Wang et al.<sup>30</sup> had previously shown that RGS4 specifically regulates delta-opioid receptor (DOP) signaling while having little to no effect on mu-opioid receptor (MOP) signaling. CCG-50014 significantly potentiates SNC-80 effects on cAMP accumulation through DOP (Figure 3C). Consistent with the previously determined specificity of RGS4, there was no significant effect of the compound on MOP-regulated cAMP levels though a trend toward potentiation of morphine activity was observed. It is not clear if this is due to effects on RGS4 or on other RGS proteins in the SH-SY5Y cells to regulate the MOP signal transduction cascade. These cellular studies demonstrate that CCG-203769 can potentiate RGS4-regulated signaling pathways, regardless of whether they are  $G\alpha_o$ - or  $G\alpha_q$ -mediated processes.

Although the TDZD inhibitors have cellular activity, specificity is always a key question regarding compounds with a covalent mechanism of action. As noted above, CCG-203769 has low potency against GSK-3 $\beta$  as well as producing no inhibition of the activity of the thiol-protease papain at 30  $\mu$ M. We also assessed off-target effects through broad activity profiling at the NIMH PDSP program (University of North Carolina, Chapel Hill).<sup>31</sup> The compound showed no activity at 10  $\mu$ M against a series of receptors, transporters, etc. (Table 2). CCG-203769 had modest activity to inhibit ligand binding in membrane preparations for a small subset of the tested systems ( $\alpha_2$  adrenergic, D3 dopamine, and opioid receptors). Using the GlowSensor assay<sup>32,33</sup> for inhibition of cAMP in cells by these  $G\alpha_{i/o}$ -coupled receptors, the TDZD compounds showed no agonist or antagonist activity at concentrations up to 10  $\mu$ M in cells (Table 2).

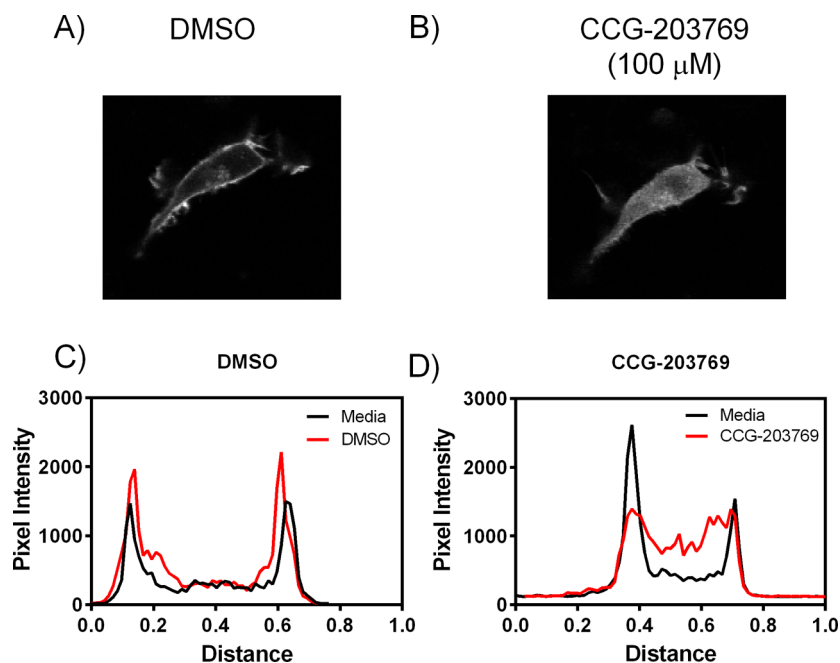


**Figure 2.** CCG-203769 inhibits the  $G\alpha_o$ -dependent membrane translocation of RGS4 in HEK293T cells. RGS4-GFP generally has a diffuse cytosolic protein expression pattern; however, coexpression with  $G\alpha_o$  induces a translocation of the RGS to the cell membrane.<sup>25</sup> (A,C) Treatment with DMSO does not modulate the RGS4 membrane localization, while (B,D) treatment with CCG-203769 (100  $\mu$ M) reverses the membrane translocation of the RGS4. Representative data shown from at least three independent experiments with 3–5 cells imaged per experiment. Line scans (C and D) were quantified from a single line perpendicular to the long axis of the cell in pre (media) and post (DMSO or CCG-203769) treatment images. Pixel intensity was obtained using the NIH ImageJ software, version 1.43r.

A critical step toward translation of new therapeutics is the demonstration of *in vivo* activity as well as avoidance of off-target effects. RGS4 is expressed in the sino-atrial node where it functions to regulate heart rate. Accordingly, RGS4 knockout mice show enhanced carbachol-induced bradycardia.<sup>34</sup> To determine whether this genetic disruption of RGS4 function could be replicated pharmacologically, we tested CCG-203769 for effects on carbachol-mediated bradycardia in conscious, unrestrained rats. Carbachol (0.1 mg/kg, IP) produces a modest decrease in heart rate (Figure 4) compared to that of a saline vehicle control. CCG-203769 (10 mg/kg, IV) had no significant effect upon heart rate when given alone (Figure 4). However, CCG-203769, administered immediately prior to carbachol, significantly potentiated the bradycardic effect (Figure 4,  $p < 0.05$ , 2-way ANOVA).

Given the functional role of RGS4 in Parkinson's disease models,<sup>15</sup> we tested CCG-203769 in a pharmacologic model of D2 antagonist-induced bradykinesia. Raclopride administration in rats causes increased hang time in the bar test (Figure 5A), which was rapidly reversed by doses of CCG-203769 ranging from 0.1 to 10 mg/kg. The lowest dose, 0.01 mg/kg had no effect, while 0.1 mg/kg produced a submaximal effect. The higher doses, 1 and 10 mg/kg, produced equivalent effects. Similarly, the raclopride-induced paw drag in mice (as indicated by the reduced numbers of steps), was reversed by 0.1–10 mg/kg CCG-203769 (Figure 5B).

In this article, we have characterized the first TDZD RGS inhibitor with physiological activity. CCG-203769 has nanomolar potency against RGS4 and RGS19 *in vitro* and is almost 5000-fold selective for RGS4 over the closely related RGS8, making CCG-203769 the most selective RGS4 inhibitor identified to date. As expected, cellular activity is less potent with half-maximal effects occurring in the 1–3  $\mu$ M range in

cells. The inducible RGS4 system provided us with strong evidence of actions on RGS4 rather than other mechanisms that could also result in potentiation of the M3 muscarinic signaling response (e.g., M3 muscarinic allosteric modulation or effects on cellular  $Ca^{2+}$  handling). There are, however, additional actions of CCG-203769 at higher concentrations that are not fully understood.

Despite its cysteine-reactive mechanism of action, CCG-203769 selectively targets RGS4 over the known TDZD target GSK3 $\beta$ , the cysteine protease papain, and a large number of receptors, and ion channels. The mechanism underlying the RGS selectivity of this compound over other cysteine-dependent processes has yet to be fully elucidated; however, the available data allow for a potential explanation. We previously showed that the covalent modification of RGS4 was through the opening of the thiazolidinone ring to form a disulfide bond with cysteine residues on the protein.<sup>25,26</sup> This reactivity would presumably provide a nonspecific mechanism of action. However, dynamic modeling studies<sup>35</sup> indicate that the target cysteines on RGS4 are buried in a hydrophobic environment that is only transiently accessible to solvent. This suggests that the cysteines in RGS4 may be in a unique environment that facilitates the high potency of CCG-203769. Also, in the reducing environment of the cell, the disulfide-bonded compound interaction is likely reversible, as shown *in vitro* with the addition of reducing agents.<sup>25</sup> Further studies are required to confirm these hypotheses.

In this article, we show that a TDZD RGS4 inhibitor, despite a covalent mechanism of action, is very selective for RGS4 over other RGS proteins as well as over other sulfhydryl-dependent enzymes and a wide range of CNS receptors. Furthermore, it has *in vivo* activity on the RGS4-dependent control of heart rate and produces beneficial effects in a D2 antagonist-mediated

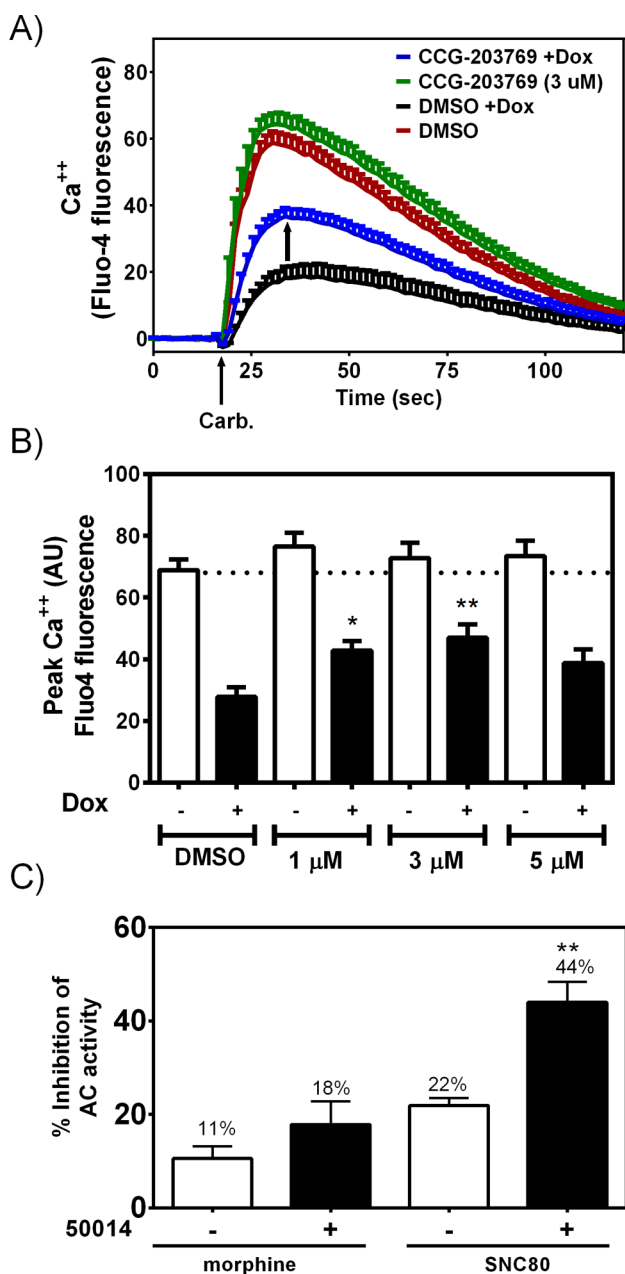


**Figure 3.** TDZD RGS4 inhibitors block RGS function in living cells. (A) RGS4 induction by doxycycline suppresses the  $G\alpha_q$ -mediated calcium transient invoked by activation of the M3 muscarinic receptor. CCG-203769 (3  $\mu$ M) reverses the effect of RGS4. (B) Quantification of the data shown in A, showing that CCG-203769 significantly inhibits the RGS4 modulation M3 signaling at 1 and 3  $\mu$ M. Data are presented as the mean  $\pm$  SEM of three independent experiments. (C)  $\delta$ -opioid receptor signaling in SH-SY5Y neuroblastoma cells is potentiated by the TDZD RGS4 inhibitor. The endogenous  $\delta$  and  $\mu$  receptors in SH-SY5Y cells are regulated by endogenous RGS proteins. CCG-50014 (100  $\mu$ M) significantly potentiates the cAMP inhibition produced by the  $\delta$  opioid receptor agonist SNC-80, while only modestly potentiating actions of the  $\mu$ -opioid receptor agonist morphine. Data are presented as the mean  $\pm$  SEM of three independent experiments. \* $p$  < 0.05; \*\* $p$  < 0.01.

akinesia and bradykinesia. In conjunction with the genetic evidence that RGS4 knockout mice have reduced defects after 6-hydroxy dopamine injury,<sup>15</sup> these results suggest that CCG-

203769 and other related RGS4 inhibitors may have potential as novel anti-Parkinsonian therapies.

## METHODS

**Sources.** Compounds were obtained from sources previously reported for carbachol;<sup>36</sup> doxycycline, [ $\gamma$ -<sup>32</sup>P] GTP;<sup>25</sup> and forskolin, morphine, and SNC80.<sup>30</sup> Raclopride was purchased from Tocris Bioscience (Bristol, UK). CCG-203769 and CCG-50014 were synthesized as previously described.<sup>26</sup> Fluo4 NW kits were obtained from Invitrogen (Carlsbad, CA). RGS proteins and  $G\alpha$  subunits were expressed, purified, and labeled as previously described.<sup>37</sup> GSK-3 $\beta$  was obtained from Sigma (catalog #G1663). HEK-293T cells expressing the M3 muscarinic receptor and inducible RGS4 (M3-R4 cells) were described previously.<sup>38</sup>

**RGS/ $G\alpha$  Binding Studies.** The binding of biotinylated RGS proteins to fluorescently labeled  $G\alpha$ , and the reversibility of RGS4 inhibitor compound actions were measured by FCPIA as previously described.<sup>37,39,40</sup>

**Single-Turnover GAP Assay.** Single turnover GTPase acceleration experiments were performed as previously described using purified His<sub>6</sub>-tagged  $G\alpha$ .<sup>25</sup>

**Steady-State GAP Assay.** Steady-state hydrolysis of unlabeled GTP was measured using malachite green in a receptor-independent assay utilizing a mutant  $G\alpha_i$  (R178M, A326S).<sup>38,41</sup> These mutations facilitate the release of GDP from the enzyme making the GTP hydrolysis step rate-limiting.<sup>41</sup> GTP hydrolysis was measured by mixing 6  $\mu$ M mutant  $G\alpha_i$  with 300  $\mu$ M GTP in 100  $\mu$ L in 96-well plates in the presence or absence of 200 nM RGS4 and CCG-203769 or DMSO (vehicle control). All assay components were diluted in a buffer comprising 50 mM HEPES at pH 7.4, 100 mM NaCl, 0.01% Lubrol, 5 mM MgCl, and 10  $\mu$ g/mL BSA. The reaction was allowed to proceed for 2 h at room temperature and then was quenched with 60  $\mu$ L of an HCl/malachite green dye solution. Immediately after the addition of malachite green, 10  $\mu$ L of 32% w/v sodium citrate was added as a colorimetric stabilizer, followed by incubation at room temperature for 20 min. Released inorganic phosphate was measured as an increase in absorbance ( $A_{630}$ ) from the complex of phosphate with malachite green.<sup>42</sup> Background control samples lacking  $G\alpha$  were used to determine the rate of nonenzymatic GTP hydrolysis which was subtracted.

**Papain Inhibition.** Experiments were performed using fluorescein-isothiocyanate-labeled casein as the fluorescent substrate as previously described.<sup>25</sup>

**GSK-3 $\beta$  Inhibition.** Purified GSK-3 $\beta$  (0.5 U, Sigma G1663) was incubated with the indicated concentration of compound for 15 min at room temperature. Substrate peptide (300 nM, Enzo #BML-P151) was added along with 1 mM [ $\gamma$ -<sup>32</sup>P] ATP. After a 15 min of incubation at 30  $^{\circ}$ C, the reaction was quenched by the addition of 4 mL of 1% phosphoric acid. The amount of phosphorylated peptide was determined by filtration on P81 phosphocellulose filters, which were washed three times with 4 mL of 1% phosphoric acid to remove unincorporated radioactivity. Incorporated radionuclide was quantified by liquid scintillation counting.

**Opioid Inhibition of Cellular cAMP.** SH-SY5Y cells were grown in DMEM containing 10% fetal bovine serum and penicillin (100 units/mL)—streptomycin (100  $\mu$ g/mL) under 5% CO<sub>2</sub> at 37  $^{\circ}$ C. Cells were plated into 24-well plates to reach  $\sim$ 90% confluency on the day of assay and washed once with fresh serum-free medium. Medium was replaced with 1 mM IBMX (3-isobutyl-1-methylxanthine) in serum-free medium for 15 min at 37  $^{\circ}$ C and then changed to medium containing 1 mM IBMX, 30  $\mu$ M forskolin, and 100 nM of either morphine or SNC80 with or without test compound for 5 min at 37  $^{\circ}$ C. Reactions were stopped by replacing the medium with ice-cold 3% perchloric acid, and samples were kept at 4  $^{\circ}$ C for at least 30 min. An aliquot (0.4 mL) from each sample was removed, neutralized with 0.08 mL of 2.5 M KHCO<sub>3</sub>, vortexed, and centrifuged at 15,000g for 1 min to pellet the precipitates. Accumulated cAMP in a 10–15  $\mu$ L aliquot of the supernatant from each sample was measured by radioimmunoassay following the manufacturer's instructions (cAMP radioimmunoassay

Table 2. Specificity Analysis of CCG-203769<sup>a</sup>

target	biochemical assays		cellular assays
	primary binding (% inhibition at 10 $\mu$ M)	secondary binding (IC <sub>50</sub> nM)	agonist/antagonist potency (EC <sub>50</sub> /IC <sub>50</sub> nM)
5-HT1A,B,D,E; 5-HT2A,B,C, 3, 5A, 7 $\beta$ -AR1,2,3; $\alpha$ 1-AR A, B, D D2, D4, H1–4; M1–5; benzodiazepine; GABA-A; DAT, NET, SERTSigma1,2	<50%	ND <sup>b</sup>	ND
5-HT6	69	>10,000	ND
$\alpha$ 2A adrenergic	97	290	>10,000
$\alpha$ 2B adrenergic	93	2,290	>10,000
$\alpha$ 2C adrenergic	97	140	>10,000
D1 dopamine	54	>10,000	ND
D3 dopamine	84	1,530	>10,000
D5 dopamine	67	>10,000	ND
DOR	53	2,630	>10,000
KOR	90	1,520	>10,000
MOR	54	2,680	>10,000

<sup>a</sup>The compound was tested for activity in a wide variety of ligand binding or functional assays through the NIH PDSP laboratory. Targets for which activity was found in primary or secondary binding assays were then examined in cell-based functional studies. In the latter, assessment of both agonist and antagonist activity was done. Assay protocols are available on the PDSP web site (<https://pdspdb.unc.edu>). <sup>b</sup>ND = Not determined.

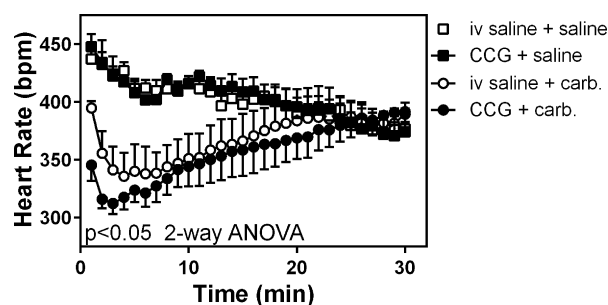


**Figure 4.** CCG-203769 potentiates the cardiovascular effects of carbachol in conscious rats. Blood pressure and heart rate of adult Sprague–Dawley rats were monitored via indwelling cardiac transponders. Rats were given CCG-203769 (10 mg/kg, i.v.) or saline immediately before the administration of saline or carbachol (0.1 mg/kg, i.p.). CCG-203769 has no effect on heart rate when administered alone; however, it significantly potentiates ( $p < 0.05$ , 2-way ANOVA) the effect of carbachol (0.1 mg/kg).  $N = 6$  per condition.

kit, GE Healthcare, Piscataway, NJ). Data are from four separate experiments, each carried out in duplicate and calculated as percent inhibition. The basal cAMP accumulation with forskolin alone with or without CCG-50014 did not differ.

**Calcium Signaling Transients.** The M3-R4 cell line with regulated expression of RGS4<sup>38</sup> was based upon the HEK-293 Flp-In T-REx cell line (Invitrogen, Carlsbad, CA). It stably expresses the muscarinic M3 receptor and has human RGS4 (stabilized C2S mutant, C-terminal HA tagged) expression under doxycycline control. Cells were maintained in DMEM supplemented with 10% fetal bovine serum and penicillin (100 units/mL)–streptomycin (100  $\mu$ g/mL) under 5% CO<sub>2</sub> at 37 °C. For experiments, cells were split into 96-well black, clear bottomed, poly-D-lysine coated microtiter plates (Nunc, Cat. # 152037) at a density of 20,000 cells/well in DMEM containing 10% fetal bovine serum and penicillin (100 units/mL)–streptomycin (100  $\mu$ g/mL). RGS4 expression was induced by supplementing the medium with 1  $\mu$ g/mL doxycycline for 24–48 h before experimentation. Cells were loaded with Fluo-4 No-Wash dye (Invitrogen, Carlsbad, CA) in loading buffer for 30 min at 37 °C. Compounds were then added and incubated for 30 min at room temperature prior to carbachol stimulation. Plates were transferred to a FlexStation 3 plate reader (Molecular Devices, Sunnyvale, CA), and carbachol (1 nM final) was injected into the wells, and the fluorescence intensity was measured as a function of time. Peak fluorescence intensity was

calculated from a 120 s kinetic measurement as a percent increase above the initial fluorescence during the preinjection period.

**RGS4 Membrane Localization.** Assays were performed as previously described.<sup>25</sup> Briefly, HEK-293T were cells grown to 80–90% confluency in 6-well dishes in DMEM supplemented with 10% fetal bovine serum and penicillin (100 units/mL)–streptomycin (100  $\mu$ g/mL) under 5% CO<sub>2</sub> at 37 °C. RGS and G $\alpha_o$  were transiently cotransfected (250 ng of a plasmid encoding full-length human RGS4 with a C-terminal GFP fusion RGS4pDEST47 and 250 ng of pcDNA3.1 or pcDNA3.1 encoding wild-type human G $\alpha_o$ ). Transfected cells were split onto poly-D-lysine coated glass coverslips and cultured for 24–48 h before live cell imaging. Images were acquired on an Olympus Fluoview 500 confocal microscope with a 60  $\times$  1.40 numerical aperture oil objective. Images were obtained by taking a series of stacks every 0.5  $\mu$ m through the cell and combined into a composite image. The light source for the fluorescence studies was a 488 nm laser with a 505–525 nm bandpass filter. Images were quantified using NIH ImageJ software, version 1.43r.

**Activity Profiling of CCG-203769.** Detailed assay protocols for primary and secondary radioligand binding studies as well as functional cell-based assays can be found on the PDSP Web site: <http://pdsp.med.unc.edu/>.

**Carbachol-Induced Bradycardia.** These studies were reviewed and approved by the University Committee on Use and Care of Animals at the University of Michigan. Under ketamine (90 mg/kg, i.p.) and xylazine (10 mg/kg, i.p.) anesthesia, rats were implanted with indwelling venous catheters (Micro-Renathane tubing, Braintree Scientific Inc., Braintree, MA, USA) and telemetric BP and ECG transmitters (Model C50-PXT, Data Sciences, Transoma Medical, Inc., St. Paul, MN, USA) at the same time under aseptic conditions. Venous catheters were inserted 3 cm into the right or left jugular vein and sutured to the vein and to the surrounding tissue at 3–4 points to secure catheter placement. The remaining tubing (approximately 9–12 cm) was threaded subcutaneously to a dorsal incision and held in place by suture to musculature directly below the incision. Telemeters were implanted subcutaneously in the rat and secured to the abdominal wall. The catheter extending from the base of the transmitter was placed 3 cm into the left femoral artery. Electrodes from the bottom of the transmitter were threaded subcutaneously, and one was sutured to the muscle above the xiphoid process, and the other was sutured to the right of the clavicle. All rats were singly housed and allowed at least 7 days to recover before testing.

The telemetry system consisted of battery-operated transmitters and receivers (Data Sciences, TransomaMedical, St. Paul, MN, USA). Mean arterial pressure (MAP) and heart rate (beats per min, bpm) were acquired using Dataquest A.R.T. 3.01, collected every 10 s and

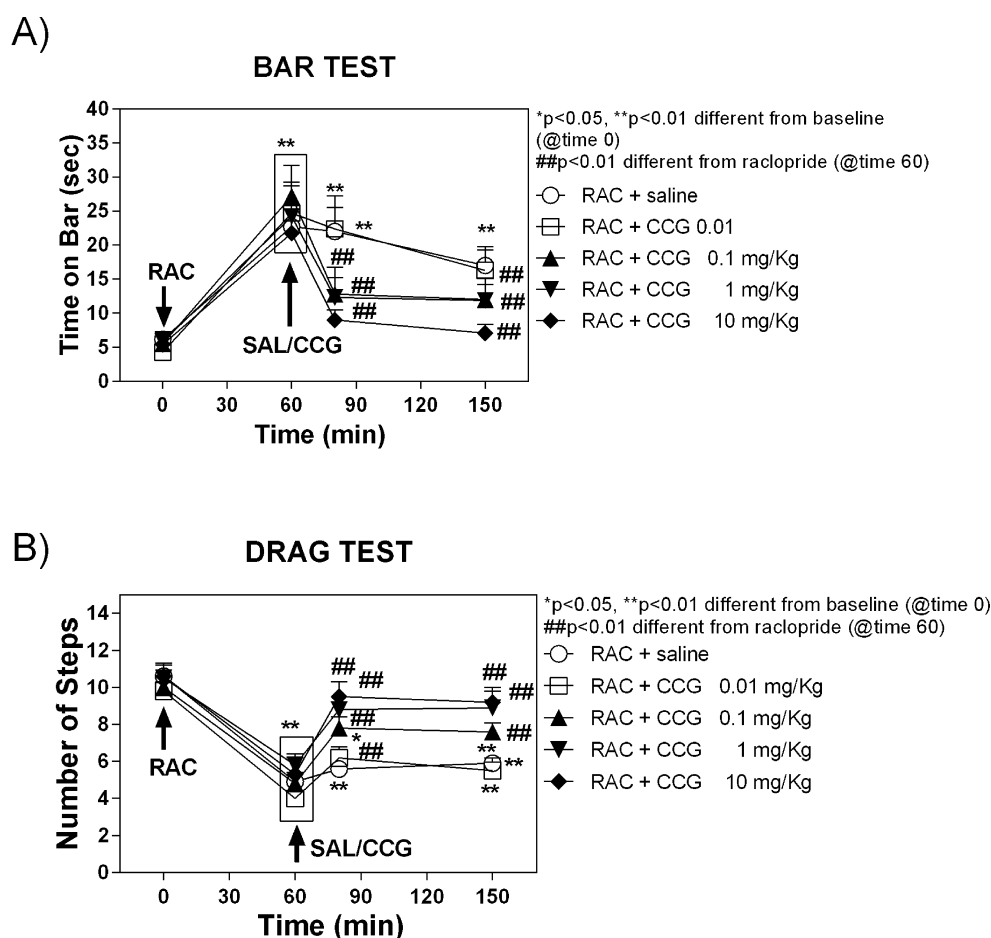


**Figure 5.** AntiParkinson's effects of RGS4 inhibitors. Mice were treated with raclopride (1 mg/kg i.p.) after baseline assessment in the bar and drag tests (as described in Methods). (A) Akinesia and (B) bradykinesia were assessed 30 min after raclopride, then mice received either DMSO or CCG-203769 at the indicated doses (i.p.). Behavior was assessed 20 or 90 min after DMSO or CCG-203769. Values are the mean  $\pm$  SEM with differences from baseline indicated by \*\* ( $p < 0.01$ ) and differences from raclopride + DMSO indicated by ## ( $p < 0.01$ ).

then averaged over 1 min periods. A rat's home cage was placed in the receiver at least 1 h prior to testing to allow for habituation. CCG-203769 is an oil and was solubilized in sterile saline by vigorous vortexing. All compounds were administered *in vivo* in a volume of 1 mL/kg by routes of administration indicated above. After habituation, rats received CCG-203769 or saline (by i.v. infusion through the indwelling venous catheter over 30 s) while freely moving in their homecage. One minute later, saline or 0.1 mg/kg carbachol (i.p.) was administered. Before and after i.v. infusions, catheters were flushed with approximately 0.5 mL of heparinized saline (50 U/mL) to check catheter patency and flush treatments from the dead space in the catheter. Following all experiments, rats were euthanized by i.v. pentobarbital (150 mg/kg) to ensure catheter patency. Statistical significance was evaluated by 2-way ANOVA with a significance cutoff of 0.05.

**Raclopride-Induced Movement Suppression.** These experimental protocols were approved by the Italian Ministry of Health (license n. 171/2010-B) and Ethical Committee of the University of Ferrara. Young male (20–25 g; 8–9 weeks) C57BL/6J mice, were purchased from Harlan Italy (S. Pietro al Natisone, Italy) and were housed with free access to food and water with a 12-h light/dark cycle with lights on between 07:00 and 19:00. Prior to pharmacological testing, mice were handled for 1 week by the same operator to reduce stress and trained daily for a week on the behavioral tests until their motor performance became reproducible. On the day of the experiment, drugs were administered systemically (i.p.); CCG-203769 was administered 30 min after raclopride.

Motor activity was evaluated by means of different behavioral tests (bar and drag) specific for different motor abilities, as previously

described.<sup>43,44</sup> The different tests are useful to evaluate motor functions under static or dynamic conditions. Akinesia appears as an abnormal absence or poverty of movements that is associated with the loss of the ability to move the forepaw when placed on blocks (bar test). Bradykinesia is slowness of movement with difficulties of adjusting in response to backward dragging (drag test). The tests were repeated in a fixed sequence (bar and drag test) before (control session) and after (30 min) raclopride injection, then 20 and 90 min after CCG-203769 injection.

The bar test or catalepsy test,<sup>45</sup> measures the ability of the animal to respond to an externally imposed static posture. Each mouse was placed gently on a table and the right and left forepaws were placed alternately on blocks of increasing heights (1.5, 3, and 6 cm). The immobility time (in seconds) on the blocks was recorded (cutoff time 20 s per step, 60 s maximum). Time was recorded as total time spent on the blocks. The drag test is a modification of the "wheelbarrow" test.<sup>46</sup> Each mouse was gently lifted by the tail (allowing the forepaws on the table) and dragged backward at a constant speed (about 20 cm/s) for a fixed distance (100 cm). The number of touches made by each forepaw was counted by two separate observers (mean between the two forepaws).

Data are expressed as the means  $\pm$  SEM of  $n$  determinations per group. Statistical analysis was performed using one-way repeated measures (RM) ANOVA followed by the Newman–Keuls test.  $P$  values  $< 0.05$  were considered to be statistically significant. Both raclopride and CCG-203769 were freshly dissolved in the vehicle just prior to use.

## ■ ASSOCIATED CONTENT

### ■ Supporting Information

Brief characterization of the M3-R4 Flp-in cell line. This material is available free of charge via the Internet at <http://pubs.acs.org>.

## ■ AUTHOR INFORMATION

### Corresponding Author

\*Department of Pharmacology & Toxicology, Michigan State University, B440 Life Sciences, 1355 Bogue St., East Lansing, MI 48824. Phone: 517 353-7145. Fax: 517 353-8915. E-mail: [rneubig@msu.edu](mailto:rneubig@msu.edu).

### Author Contributions

L.B., A.S., and S.W. designed and performed the biochemical and cell-based assays. Q.W. and J.T. designed the opioid functional studies which were performed by Q.W. E.J. and L.B. designed and performed the studies on compound effects on muscarinic bradycardia. E.T. and S.H. designed and synthesized CCG-203769. M.C. and M.M. designed and M.C. performed the Parkinson's model studies. X.-P.H. designed and performed the target screening studies at the PDSP. R.N. contributed to the design of the overall project and all individual experiments. R.N. and L.B. wrote the manuscript with text and suggestions contributed by all authors.

### Funding

Funding was provided by NIH RO1 DA023252 (to R.R.N.), the Chemical Biology Interface training program (NIH T32GM008597) (to L.L.B.) and core facilities supported by the Michigan Diabetes Research and Training Center (NIH P60 DK020572), and University of Michigan Comprehensive Cancer Center Support Grant NIH P30 CA046592.

### Notes

The authors declare the following competing financial interest(s): Richard Neubig is founder and owner of Argessin LLC which has licensed rights to TDZD RGS4 inhibitors from the University of Michigan.

## ■ ACKNOWLEDGMENTS

We thank Jian Mei for assistance with the FCPIA studies and Roger Sunahara and John Tesmer for valuable discussions. Receptor binding profiles and agonist and antagonist functional data were generously provided by the National Institute of Mental Health's Psychoactive Drug Screening Program, Contract # HHSN-271-2013-00017-C (NIMH PDSP). The NIMH PDSP is directed by Bryan L. Roth MD, Ph.D. at the University of North Carolina at Chapel Hill and Project Officer Jamie Driscoll at NIMH, Bethesda MD, USA. For experimental details please refer to the PDSP web site <http://pdsp.med.unc.edu/>.

## ■ REFERENCES

(1) Carrieri, A., Perez-Nueno, V. I., Lentini, G., and Ritchie, D. W. (2013) Recent trends and future prospects in computational GPCR drug discovery: from virtual screening to polypharmacology. *Curr. Top. Med. Chem.* 13, 1069–1097.

(2) Nickols, H. H., and Conn, P. J. (2014) Development of allosteric modulators of GPCRs for treatment of CNS disorders. *Neurobiol. Dis.* 61, 55–71.

(3) Shonberg, J., Lopez, L., Scammells, P. J., Christopoulos, A., Capuano, B., and Lane, J. R. (2014) Biased agonism at G protein-coupled receptors: The promise and the challenges - A medicinal chemistry perspective. *Med. Res. Rev.* 34, 1286–1330.

(4) Congreve, M., Dias, J. M., and Marshall, F. H. (2014) Structure-based drug design for G protein-coupled receptors. *Prog. Med. Chem.* 53, 1–63.

(5) Hollenstein, K., de Graaf, C., Bortolato, A., Wang, M. W., Marshall, F. H., and Stevens, R. C. (2014) Insights into the structure of class B GPCRs. *Trends Pharmacol. Sci.* 35, 12–22.

(6) Christopoulos, A. (2014) Advances in G protein-coupled receptor allosterity: From function to structure. *Mol. Pharmacol.* 86, 463–478.

(7) Blazer, L. L., and Neubig, R. R. (2009) Small molecule protein-protein interaction inhibitors as CNS therapeutic agents: current progress and future hurdles. *Neuropsychopharmacology* 34, 126–141.

(8) Neubig, R. R., and Siderovski, D. P. (2002) Regulators of G-protein signalling as new central nervous system drug targets. *Nat. Rev. Drug Discovery* 1, 187–197.

(9) Sjogren, B., Blazer, L. L., and Neubig, R. R. (2010) Regulators of G protein signaling proteins as targets for drug discovery. *Prog. Mol. Biol. Transl. Sci.* 91, 81–119.

(10) Traynor, J. R., and Neubig, R. R. (2005) Regulators of G protein signaling & drugs of abuse. *Mol. Interventions* 5, 30–41.

(11) Bodle, C. R., Mackie, D. I., and Roman, D. L. (2013) RGS17: an emerging therapeutic target for lung and prostate cancers. *Future Med. Chem.* 5, 995–1007.

(12) Kimple, A. J., Bosch, D. E., Giguere, P. M., and Siderovski, D. P. (2011) Regulators of G-protein signaling and their Galpha substrates: promises and challenges in their use as drug discovery targets. *Pharmacol. Rev.* 63, 728–749.

(13) Sjogren, B. (2011) Regulator of G protein signaling proteins as drug targets: current state and future possibilities. *Adv. Pharmacol.* 62, 315–347.

(14) Chen, Y., Liu, Y., Cottingham, C., McMahon, L., Jiao, K., Greengard, P., and Wang, Q. (2012) Neurabin scaffolding of adenosine receptor and RGS4 regulates anti-seizure effect of endogenous adenosine. *J. Neurosci.* 32, 2683–2695.

(15) Lerner, T. N., and Kreitzer, A. C. (2012) RGS4 is required for dopaminergic control of striatal LTD and susceptibility to Parkinsonian motor deficits. *Neuron* 73, 347–359.

(16) Ko, W. K., Martin-Negrier, M. L., Bezard, E., Crossman, A. R., and Ravenscroft, P. (2014) RGS4 is involved in the generation of abnormal involuntary movements in the unilateral 6-OHDA-lesioned rat model of Parkinson's disease. *Neurobiol. Dis.* 70, 138–148.

(17) Azzarito, V., Long, K., Murphy, N. S., and Wilson, A. J. (2013) Inhibition of alpha-helix-mediated protein-protein interactions using designed molecules. *Nat. Chem.* 5, 161–173.

(18) London, N., Raveh, B., and Schueler-Furman, O. (2013) Druggable protein-protein interactions—from hot spots to hot segments. *Curr. Opin. Chem. Biol.* 17, 952–959.

(19) Voet, A., Banwell, E. F., Sahu, K. K., Heddl, J. G., and Zhang, K. Y. (2013) Protein interface pharmacophore mapping tools for small molecule protein: protein interaction inhibitor discovery. *Curr. Top. Med. Chem.* 13, 989–1001.

(20) Morelli, X., Bourgeois, R., and Roche, P. (2011) Chemical and structural lessons from recent successes in protein-protein interaction inhibition (2P2I). *Curr. Opin. Chem. Biol.* 15, 475–481.

(21) Mullard, A. (2012) Protein-protein interaction inhibitors get into the groove. *Nat. Rev. Drug Discovery* 11, 173–175.

(22) Villoutreix, B. O., Labbe, C. M., Lagorce, D., Laconde, G., and Sperandio, O. (2012) A leap into the chemical space of protein-protein interaction inhibitors. *Curr. Pharm. Des.* 18, 4648–4667.

(23) Kalgutkar, A. S., and Dalvie, D. K. (2012) Drug discovery for a new generation of covalent drugs. *Expert Opin. Drug Discovery* 7, 561–581.

(24) Lopez-Tarruella, S., Jerez, Y., Marquez-Rodas, I., and Martin, M. (2012) Neratinib (HKI-272) in the treatment of breast cancer. *Future Oncol.* 8, 671–681.

(25) Blazer, L. L., Zhang, H., Casey, E. M., Husbands, S. M., and Neubig, R. R. (2011) A nanomolar-potency small molecule inhibitor of regulator of G protein signaling (RGS) proteins. *Biochemistry* 50, 3181–3192.

- (26) Turner, E. M., Blazer, L. L., Neubig, R. R., and Husbands, S. M. (2012) Small molecule inhibitors of regulator of G protein signalling (RGS) proteins. *ACS Med. Chem. Lett.* 3, 146–150.
- (27) Rosa, A. O., Kaster, M. P., Binfare, R. W., Morales, S., Martin-Aparicio, E., Navarro-Rico, M. L., Martinez, A., Medina, M., Garcia, A. G., Lopez, M. G., and Rodrigues, A. L. (2008) Antidepressant-like effect of the novel thiazolidinone NP031115 in mice. *Prog. Neuropsychopharmacol. Biol. Psychiatry* 32, 1549–1556.
- (28) Castro, A., Encinas, A., Gil, C., Brase, S., Porcal, W., Perez, C., Moreno, F. J., and Martinez, A. (2008) Non-ATP competitive glycogen synthase kinase 3beta (GSK-3beta) inhibitors: study of structural requirements for thiazolidinone derivatives. *Bioorg. Med. Chem.* 16, 495–510.
- (29) Martinez, A., Alonso, M., Castro, A., Perez, C., and Moreno, F. J. (2002) First non-ATP competitive glycogen synthase kinase 3 beta (GSK-3beta) inhibitors: thiazolidinones (TDZD) as potential drugs for the treatment of Alzheimer's disease. *J. Med. Chem.* 45, 1292–1299.
- (30) Wang, Q., Liu-Chen, L. Y., and Traynor, J. R. (2009) Differential modulation of mu- and delta-opioid receptor agonists by endogenous RGS4 protein in SH-SY5Y cells. *J. Biol. Chem.* 284, 18357–18367.
- (31) Besnard, J., Ruda, G. F., Setola, V., Abecassis, K., Rodriguiz, R. M., Huang, X. P., Norval, S., Sassano, M. F., Shin, A. I., Webster, L. A., Simeons, F. R., Stojanovski, L., Prat, A., Seidah, N. G., Constam, D. B., Bickerton, G. R., Read, K. D., Wetsel, W. C., Gilbert, I. H., Roth, B. L., and Hopkins, A. L. (2012) Automated design of ligands to polypharmacological profiles. *Nature* 492, 215–220.
- (32) Fenalti, G., Giguere, P. M., Katritch, V., Huang, X. P., Thompson, A. A., Cherezov, V., Roth, B. L., and Stevens, R. C. (2014) Molecular control of delta-opioid receptor signalling. *Nature* 506, 191–196.
- (33) Wu, H., Wacker, D., Mileni, M., Katritch, V., Han, G. W., Vardy, E., Liu, W., Thompson, A. A., Huang, X. P., Carroll, F. I., Mascarella, S. W., Westkaemper, R. B., Mosier, P. D., Roth, B. L., Cherezov, V., and Stevens, R. C. (2012) Structure of the human kappa-opioid receptor in complex with JDTic. *Nature* 485, 327–332.
- (34) Cifelli, C., Rose, R. A., Zhang, H., Voigtlaender-Bolz, J., Bolz, S. S., Backx, P. H., and Heximer, S. P. (2008) RGS4 regulates parasympathetic signaling and heart rate control in the sinoatrial node. *Circ. Res.* 103, 527–535.
- (35) Vashisth, H., Storaska, A. J., Neubig, R. R., and Brooks, C. L., III (2013) Conformational dynamics of a regulator of G-protein signaling protein reveals a mechanism of allosteric inhibition by a small molecule. *ACS Chem. Biol.* 8, 2778–2784.
- (36) Fu, Y., Huang, X., Zhong, H., Mortensen, R. M., D'Alecy, L. G., and Neubig, R. R. (2006) Endogenous RGS proteins and Galpha subtypes differentially control muscarinic and adenosine-mediated chronotropic effects. *Circ. Res.* 98, 659–666.
- (37) Roman, D. L., Ota, S., and Neubig, R. R. (2009) Polyplexed flow cytometry protein interaction assay: A novel high-throughput screening paradigm for RGS protein inhibitors. *J. Biomol. Screen* 14, 610–619.
- (38) Storaska, A. J., Mei, J. P., Wu, M., Li, M., Wade, S. M., Blazer, L. L., Sjogren, B., Hopkins, C. R., Lindsley, C. W., Lin, Z., Babcock, J. J., McManus, O. B., and Neubig, R. R. (2013) Reversible inhibitors of regulators of G-protein signaling identified in a high-throughput cell-based calcium signaling assay. *Cell. Signal.* 25, 2848–2855.
- (39) Blazer, L. L., Roman, D. L., Muxlow, M. R., and Neubig, R. R. (2010) Use of flow cytometric methods to quantify protein-protein interactions. *Curr. Protoc. Cytom.*, Chapter 13, Unit 13.11, pp 11–15.
- (40) Roman, D. L., Talbot, J. N., Roof, R. A., Sunahara, R. K., Traynor, J. R., and Neubig, R. R. (2007) Identification of small-molecule inhibitors of RGS4 using a high-throughput flow cytometry protein interaction assay. *Mol. Pharmacol.* 71, 169–175.
- (41) Zielinski, T., Kimple, A. J., Hutsell, S. Q., Koeff, M. D., Siderovski, D. P., and Lowery, R. G. (2009) Two Galpha(i1) rate-modifying mutations act in concert to allow receptor-independent, steady-state measurements of RGS protein activity. *J. Biomol. Screening* 14, 1195–1206.
- (42) Chang, L., Bertelsen, E. B., Wisen, S., Larsen, E. M., Zuiderweg, E. R., and Gestwicki, J. E. (2008) High-throughput screen for small molecules that modulate the ATPase activity of the molecular chaperone DnaK. *Anal. Biochem.* 372, 167–176.
- (43) Marti, M., Trapella, C., Viaro, R., and Morari, M. (2007) The nociceptin/orphanin FQ receptor antagonist J-113397 and L-DOPA additively attenuate experimental parkinsonism through overinhibition of the nigrothalamic pathway. *J. Neurosci.* 27, 1297–1307.
- (44) Viaro, R., Sanchez-Pernaute, R., Marti, M., Trapella, C., Isacson, O., and Morari, M. (2008) Nociceptin/orphanin FQ receptor blockade attenuates MPTP-induced parkinsonism. *Neurobiol. Dis.* 30, 430–438.
- (45) Sanberg, P. R., Bunsey, M. D., Giordano, M., and Norman, A. B. (1988) The catalepsy test: its ups and downs. *Behav. Neurosci.* 102, 748–759.
- (46) Schallert, T., De Ryck, M., Whishaw, I. Q., Ramirez, V. D., and Teitelbaum, P. (1979) Excessive bracing reactions and their control by atropine and L-DOPA in an animal analog of Parkinsonism. *Exp. Neurol.* 64, 33–43.